Research Article

Received: 22 December 2011 Revised: 6 April 2012 Accepted: 9 July 2012 Published online in Wiley Online Library:

(wileyonlinelibrary.com) DOI 10.1002/pi.4340

Synthesis of photoaddressable polymeric networks having azobenzene moieties and alkyl-chain-containing compounds

Antonela B Orofino, María J Galante and Patricia A Oyanguren*

Abstract

We discuss the synthesis of new optically active polymeric networks containing azobenzene moieties and different alkyl-chain-containing compounds. An epoxy resin based on diglycidyl ether of bisphenol A (DGEBA) was reacted with metaxylylenediamine (MXDA). An azo prepolymer (TAZ) was synthesized by reaction between Disperse Orange-3 and DGEBA. Reaction between palmitic acid (PA) and DGEBA was performed using triphenylphosphine as catalyst of the epoxy–acid reaction employing variable molar ratios of epoxy to carboxyl groups ($r = 1, 2, 4$). These precursors were called PA1, PA2 and PA4. Crosslinked epoxy-based azopolymers containing variable PA-based precursor content and constant chromophore concentration equal to 20 wt% TAZ were synthesized. Their reversible optical storage properties were studied and compared. It was found that the optical response is a direct consequence of the morphologies generated, and that crystallization of PA-based precursor can take place. When the PA-based precursor is not covalently bonded to the matrix, e.g. PA1, the remaining birefringence is high. PA4-modified materials present a completely different response, showing a behaviour that could be of great importance in the development of optical switchers. In this case, the organic tails remain dissolved in the matrix and unable to crystallize, giving a typical 'on–off' response.

Keywords: photoinduced anisotropy; azopolymer; epoxy networks; palmitic acid

INTRODUCTION

The aromatic azo group is of special interest because of the existence of *trans–cis* isomerism and its effect on the photochromic properties of polymers. Azobenzene-containing materials are photochromic and reversibly switch between two spectroscopically distinct forms by use of light. Thus azobenzene-based polymers are interesting due to their photoresponsive behaviour which can be utilized in optical switches, optical data recording or optical information storage.[1–6]

Assuming that an amorphous azobenzene film is irradiated by a linearly polarized beam, molecules are subjected to the *trans–cis* photoisomerization process but the *cis* form of azobenzenes substituted by donor and acceptor terminal groups easily relaxes back to the *trans* form. During this process, the molecular directions of the relaxed *trans* molecules need not coincide with those of the original state. Then, if we continue the beam excitation, *trans–cis–trans* isomerization cycles are iterated continuously. However, the molecules that lie in a direction perpendicular to the electric field of the incident excitation beam do not absorb the light because they do not have any transition dipole moment in the polarization direction of the incoming light. As a result, the molecules that align perpendicular to the electric field of the incident beam are excluded from the photoisomerization cycles; thus the population of such azobenzene molecules increases with irradiation time. This whole process is called photoinduced molecular reorientation (or photoalignment) of azobenzenes, and it generates macroscopic birefringence in the bulk (photoinduced birefringence). In particular, azobenzene-attached side-chain-type polymers are promising materials to show this phenomenon due to their optical properties, chemical and physical stability and processability.

On the other hand, liquid crystalline polymers containing azo groups on the side chain have been proposed as materials for optical storage.[7] One of the most interesting observations on these liquid crystalline polymers is that, if a mixture of mesogens is present in the side chains, the non-photoactive mesogens (such as phenyl benzoate or benzamide) undergo a reorientation together with the azo mesogens, thus amplifying the effect over the limits given by the azo groups' concentration. This effect is called cooperative orientation and has been observed in a separate study, in a series of copolymers of maleic anhydride which were semicrystalline.[8] Another way to describe this type of motion would be the motion of a chromophore under constraint.[9] The constraint can be either a liquid crystalline domain or a semicrystalline one. In this case, what happens is reorientation of the whole liquid crystalline or semicrystalline domains to a direction perpendicular to the light polarization, amplifying the phenomenon.

Accordingly, although the azobenzenes are very promising materials for rewritable holographic recording media, further improvement of the performance, such as the birefringence value, response time, long-term stability (archival life) and durability,

* *Correspondence to: Patricia A Oyanguren. E-mail: poyangur@fi.mdp.edu.ar*

Institute of Materials Science and Technology (INTEMA), University of Mar del Plata and National Research Council (CONICET), J. B. Justo 4302, 7600 Mar del Plata, Argentina

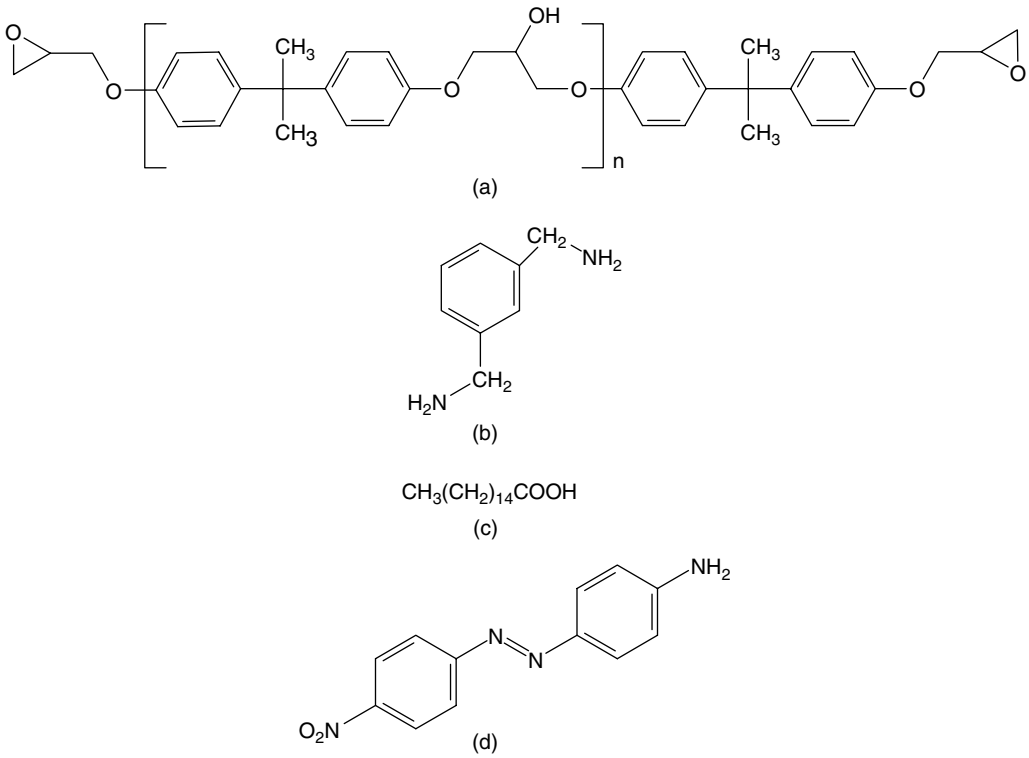

Figure 1. Chemical structure of (a) DGEBA, (b) MXDA, (c) PA and (d) DO3.

is still required for conventional azobenzene materials before they can be used in practical applications. We have previously reported the results of our investigations of photoaddressable epoxy-based azopolymers, each with distinct differences in the molecular structure of the unit building blocks.[10] We found that networks with the same chromophore concentration but different backbones exhibit similar levels of induced anisotropy under the same irradiation conditions. The remaining birefringence and relaxation times are influenced by the molecular weight between crosslinks of networks. Continuing and extending the study in this field, we present in this paper the optical response of crosslinked azobenzene polymers modified with different alkyl-containing compounds. Some of these compounds form semicrystalline domains, and we investigate their influence over the photo-orientation of the azo chromophores. We discuss to what extent the nature of the neighbouring organic molecules and the degree of union with the matrix can influence the reorientation of the azo groups, affecting the optical properties and their potential applications in optical devices.

EXPERIMENTAL

Chemicals

A push–pull azo chromophore, Disperse Orange-3 (DO3) (Sigma-Aldrich, St. Louis, USA, dye content 95%), was selected as photosensitive reactive. The bifunctional epoxy resin employed was a high purity diglycidyl ether of bisphenol A (DGEBA) (Sigma-Aldrich, St. Louis, USA, Der 332, Fluka) with a mass per mole of epoxy groups equal to 174 g mol^{-1}. The aliphatic diamine was *m*-xylylenediamine (MXDA) (Sigma Aldrich Chemie, Steinheim, Germany). The crystalline solid palmitic acid (PA) (Sigma-Aldrich, St. Louis, USA; $T_m = 63\,^{\circ}C$) was used as received. The chemical structures are shown in Fig. 1.

Synthesis of PA-based precursors

Triphenylphosphine (Fluka AG, Buchs SG, Switzerland) was used as catalyst of the epoxy–acid reaction at a concentration of 0.3 wt% for all formulations. The selected amounts of PA, DGEBA and triphenylphosphine were mixed at 90 °C until a homogeneous solution was obtained. The reaction was performed at 90 °C up to complete conversion of epoxy groups as assessed by Fourier transform infrared (FTIR) spectroscopy. Depending on the ratio of epoxy to carboxyl groups employed the complete cure took 4 h for a blend with $r = 4$, 12 h for $r = 2$ and 48 h for $r = 1$. These precursors were called PA4, PA2 and PA1, respectively. It is expected that all precursors consist of a mixture of compounds: PA-DGEBA-PA (disubstituted compound), PA-DGEBA (monosubstituted compound) and DGEBA. Figure 2 shows the scheme of the opening reaction of the epoxy group with the carboxyl group.

Synthesis of azo prepolymer

An azo prepolymer (TAZ) was synthesized by reaction between DO3 and DGEBA.[11,12] It was prepared in a stoichiometric ratio of amine (from DO3) to epoxy equivalents (from DGEBA) equal to 0.5, to generate reaction products with epoxy groups in the extreme of chains. The resulting TAZ, having a chromophore concentration per weight relative to the polymer backbone of 26 wt%, was attached to networks via the epoxy groups. The weight-average molecular weight of TAZ, determined by SEC, was 2045 g mol^{-1}.

Synthesis of azo networks

Several crosslinked epoxy-based azopolymers containing PA-based precursors were synthesized. All of them have a constant chromophore concentration equal to 5 wt% DO3 (20 wt% TAZ) and various PA-based precursor contents. Selected amounts of

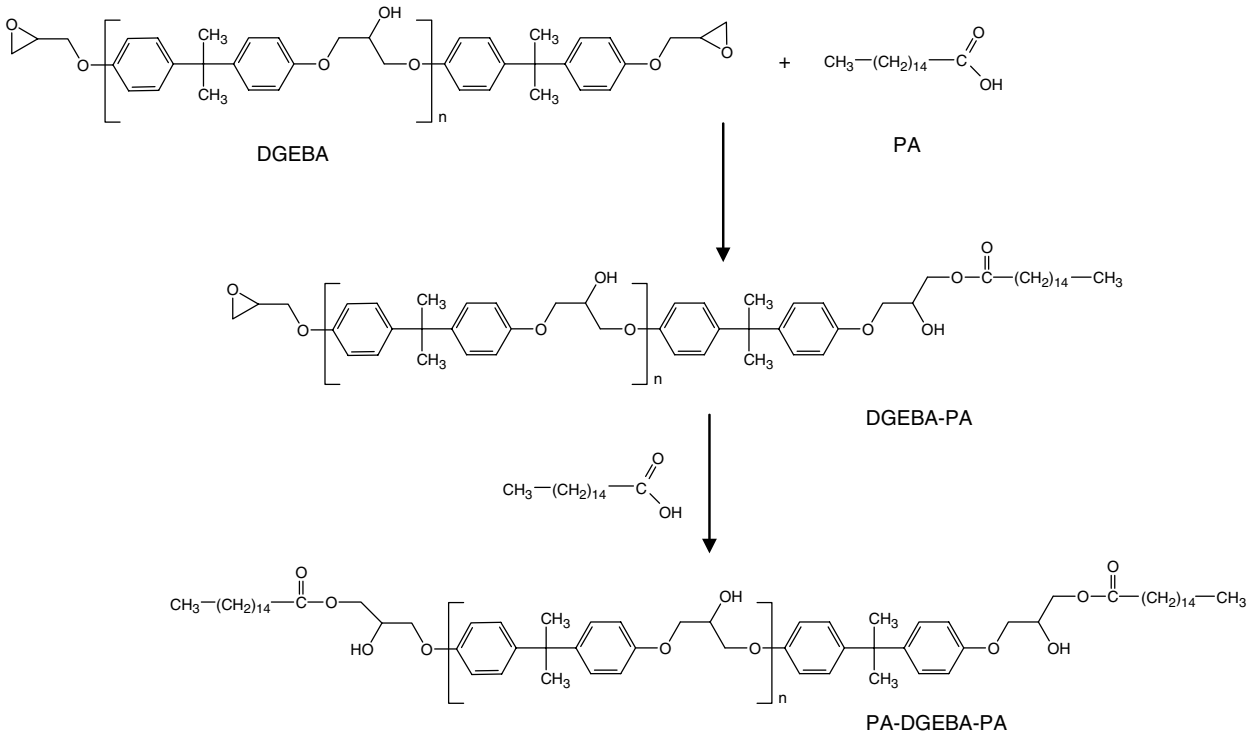

Figure 2. Scheme of the organic acid reaction with the epoxy group.

PA-based precursor and TAZ were blended with DGEBA and cured with MXDA, using a stoichiometric ratio of epoxy to amino hydrogen groups equal to 1. The curing reaction of the reactive mixtures was carried out at 100 °C for 6 h.[13] For all samples reactive mixtures were cured up to complete conversion of epoxy groups as assessed by FTIR spectroscopy. The resultant polymer networks are called PA1-TAZ-DGEBA-MXDA, PA2-TAZDGEBA-MXDA and PA4-TAZ-DGEBA-MXDA.

Characterization techniques

SEC (Knauer K-501) was used to determine the molar mass distribution of products. The device was equipped with four columns packed with styrene-divinylbenzene 5 µm copolymer particles (Phenomenex Phenogel 50 Å, 100 Å and M2, Waters Styragel 10^4 Å) and a refractive index detector (K-2301 Knauer). The mobile phase was tetrahydrofuran with an elution rate of 1 mL min^{-1}. All the scans were performed at room temperature.

The composition of the reaction products was assessed by FTIR spectroscopy. Infrared spectra were recorded on FTIR Thermo Scientific Nicolet 6700 and Genesis II Matson spectrometers at 4 and 2 cm^{-1} wavelength resolution, respectively. In all, 32 scans per slice were collected for all spectra.

DSC (Pyris 1, Perkin Elmer) was used to determine the glass transition temperature (T_g) and the melting temperature (T_m) during heating scans at 10 °C min^{-1} under nitrogen flow. T_g was defined as the onset of the transition while T_m and the crystallization temperature (T_c) were measured at the peak temperatures of the endothermic and exothermic heats, respectively. For the crystallization behaviour, samples were melted to 90 °C, held for 5 min to remove crystal memory, and then cooled to −50 °C at a cooling rate of 10 °C min^{-1}.

The overall morphology of the final materials was investigated by transmission optical microscopy (TOM) using a Leica DMLB microscope provided with a video camera (Leica DC 100); a hot stage (Linkam THMS 600) was used for this purpose.

Crystalline phases were characterized by grazing incidence X-ray diffraction on a PANalytical X'Pert powder diffractometer equipped with a graphite monochromator and a Cu anode, operating at 40 kV and 40 mA. A constant incidence angle of 1° was used and the scannings were made between 2° and 40° in 2θ.

Film preparation

All samples before reaction were dissolved in tetrahydrofuran (Biopack, 99%) at a concentration of 10–20 wt%. Films were obtained on glass substrates previously cleaned using the standard RCA method[14] by spin coating using a single wafer spin processor (model WS-400E-6NPP-lite, by Laurell). The spinner cycle programme was as follows: 1000 rpm for 30 s, 4000 rpm for 10 s, and 8000 rpm for 20 s. After curing, films were heated above their glass transition temperatures to erase any preferential orientation of the chromophores during polymerization. Samples were subsequently stored at room temperature. In some cases, the sample was kept at −20 °C for 14 days in order to examine the annealing effect on the optical behaviour of the polymer network. The thickness of each film was kept identical through using an equal amount of solution and coating an equal area. All the films had comparable thickness values, of the order of 1000 ± 100 nm. The film thickness was determined from topographic images of the scratched film obtained by AFM (5500 SPM Agilent Technologies) in contact mode.

Photoinduced birefringence measurements

Optical storage experiments were carried out at room temperature and under ambient conditions. The optical configuration for the measurement of photoinduced birefringence was similar to that previously reported.[15] The optical birefringence was induced in

the film using a linearly polarized semiconductor continuous laser operating at 488 nm (writing beam) with a polarization angle of 45° with respect to the polarization direction of the probe beam. The power of the writing beam used in the experiments was 4 mW mm^{-2} to study the time and amplitude of the optically induced birefringence. The change in the transmission of a low power semiconductor laser at 635 nm (reading beam), which passed through two crossed polarizers and the sample, was measured with a photodiode. Each photo-orientation experiment was done on a different previously non-irradiated spot so as to avoid irradiation history complications. The induced birefringence was determined by measuring the probe beam transmission ($T = I/I_0$) according to

$$\Delta n = (\lambda / \pi d) \sin^{-1} (I / I_0)^{1/2} \quad (1)$$

where λ is the wavelength of the incident radiation, d is the film thickness, I_0 is the incident beam intensity and I is the intensity after the second polarizer.

RESULTS AND DISCUSSION

PA-based precursors

The epoxy–acid chemistry is complex involving different possible reactions. In the uncatalysed reaction of epoxy groups with carboxyl groups four reaction products are to be expected.[16] The main reactions are (a) the ring opening of the epoxy group with a carboxyl group resulting in an ester bond and formation of an OH group, (b) esterification of the OH groups formed with carboxylic acid groups to a complete esterified product, (c) the reaction of the OH groups formed with epoxy groups leading to ether formation and (d) hydrolysis of the epoxy groups. The formation of ether linkages is more of a problem in the presence of an acid catalyst. Under triphenylphosphine catalysis the opening of the epoxide rings resulting in an ester bond constitutes the main reaction.[17]

Reactions taking place during the reaction of PA and DGEBA were analysed. Several formulations prepared with different molar ratios r of epoxy to carboxyl groups were studied. The FTIR spectra of monomers (DGEBA and PA) and PA-DGEBA reaction products with $r = 1$, 2 and 4 (PA1, PA2 and PA4) after reaction at 90 °C are shown in Fig. 3. The C=O group of PA exhibits an absorption band centred at 1700 cm^{-1}. After reaction, no trace of carboxyl signal remained in the FTIR spectrum shown in Fig. 3(a). The development of a new signal located at 1740 cm^{-1}, which might correspond to the stretching vibration of C=O of an ester group, is evidence that condensation took place.[18] Similarly, in the same figure is shown the stretching vibration of the OH groups formed, located at 3440 cm^{-1}. The signals corresponding to epoxy groups can be observed in Fig. 3(b). As expected, epoxy vibration signals at 915 and 863 cm^{-1} disappeared completely only for the stoichiometric sample (PA1). These results are a consequence of the condensation reaction between carboxyl groups of PA and epoxy groups of DGEBA. Furthermore, the possible reaction of epoxy homopolymerization in the presence of triphenylphosphine was studied in the near-IR region (7000–4000 cm^{-1}). Experimental results (not shown) confirmed the absence of epoxy homopolymerization under these experimental conditions.

The product distribution at the end of reaction was followed by SEC. Figure 4 shows size exclusion chromatograms of the reagents DGEBA and PA and mixtures PA1, PA2 and PA4 after reaction. The chromatogram of DGEBA shows an intensive peak at 34.5 min

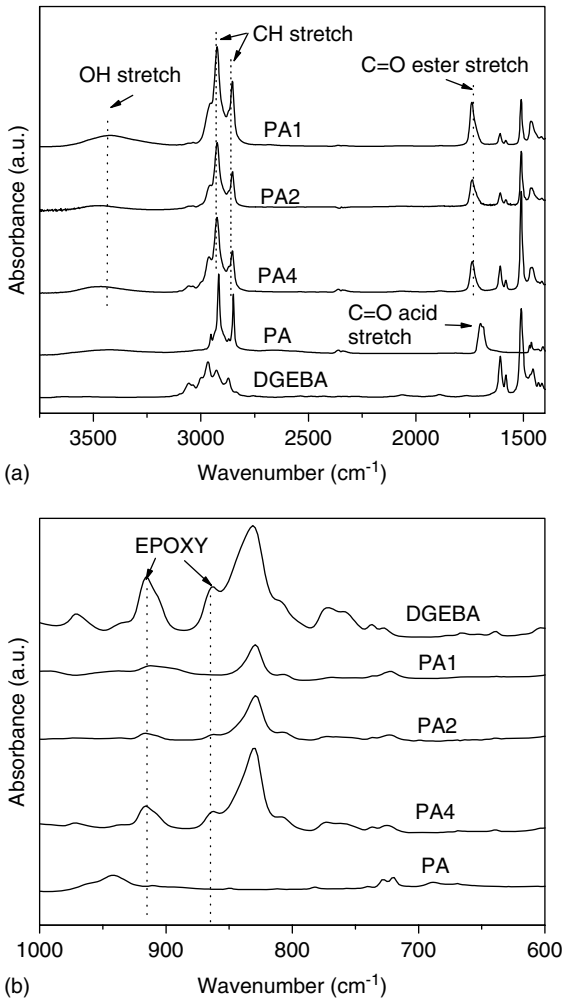

Figure 3. FTIR spectra of PA, DGEBA and PA-based precursors (PA1, PA2 and PA4) after complete reaction: (a) 3750–1700 cm^{-1} range; (b) 1000–600 cm^{-1} range.

($n = 0$), and the corresponding chromatogram for PA shows a peak located at 32.9 min. SEC traces of reaction products showed two main peaks present at retention times of 31.1 and 29.5 min, which can be assigned to the DGEBA monomer end-capped with one PA unit – DGEBA-PA (monosubstituted) – and to the disubstituted product PA-DGEBA-PA, respectively. As expected, the main product obtained for the stoichiometric formulation (PA1) is a DGEBA molecule that is reacted at both ends with PA, while the formulation with a great excess of epoxy groups (PA4) consists of monosubstituted DGEBA.

The distribution of reaction products may be estimated by assuming that the two epoxy groups have equal reactivity and there are no substitution effects. For this case, the probability of finding a reacted position is p while the probability of finding an unreacted position is $1 - p$, where p represents the stoichiometric ratio of functionalities.

This leads to the following ideal distribution of reaction products with respect to initial DGEBA molecules $(DGEBA)_0$ (summarized in Table 1):

$$DGEBA/(DGEBA)_0 = (1-p)^2$$
$$DGEBA\text{-}PA/(DGEBA)_0 = 2p(1-p)$$
$$PA\text{-}DGEBA\text{-}PA/(DGEBA)_0 = p^2$$

Table 1. Ideal and experimental molar fraction distribution of PA-based precursors after complete reaction

	PA1, $p = 1$		PA2, $p = 0.5$		PA4, $p = 0.25$	
Reaction product	Ideal	Exp.	Ideal	Exp.	Ideal	Exp.
DGEBA/$(DGEBA)_0$	0	0.03	0.25	0.26	0.56	0.58
DGEBA-PA/$(DGEBA)_0$	0	0.10	0.50	0.46	0.37	0.38
PA-DGEBA-PA/$(DGEBA)_0$	1	0.87	0.25	0.28	0.06	0.04

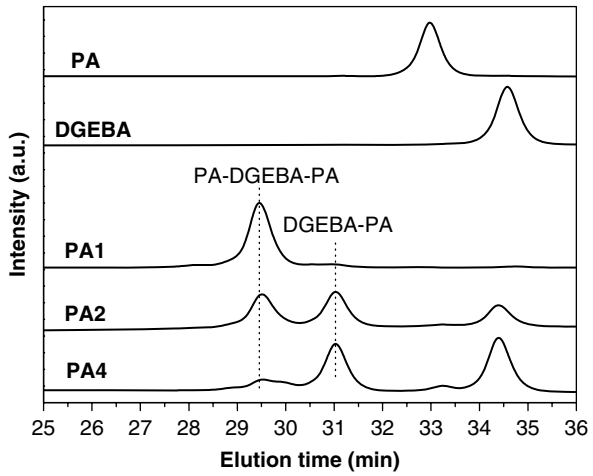

Figure 4. Size exclusion chromatograms of reactants DGEBA and PA. Also shown are the reaction product chromatograms obtained for the PA-based precursors PA1, PA2 and PA4.

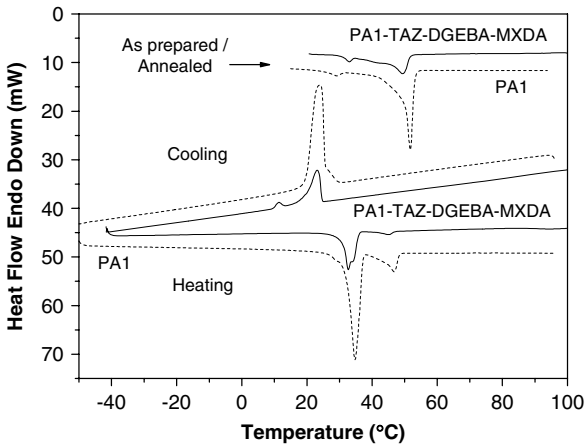

Figure 6. DSC traces for PA1 precursor (melting) and for the PA1-based network containing 20 wt% PA1 (melting and crystallization behaviour). The figure shows DSC traces for samples with different thermal histories: annealed at −20 °C for 14 days (dotted lines) and after being cooled from 100 °C (solid lines).

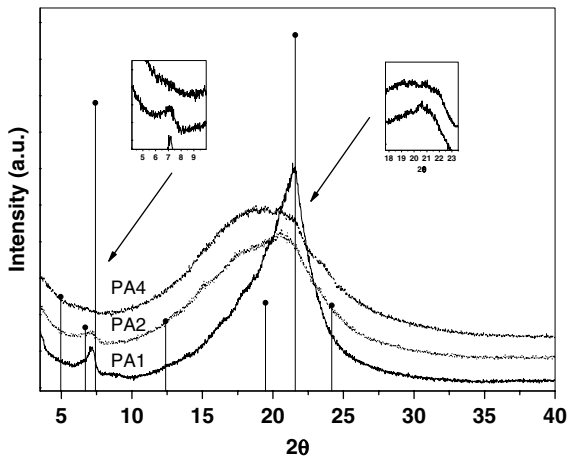

Figure 5. X-ray diffraction spectra of pure PA (main lines, the height of the lines indicates the intensity of the peaks) and PA-based precursors. The insets show an amplification of the signals at 7.17 and 21.45 2θ for PA2 and PA4.

To calculate the product distribution it was necessary to quantify each species as a function of its signal in the size exclusion chromatogram. To do this, an auxiliary factor f = signal(peak area)/(injected mass) was calculated for all the species. With the peak area of each species, f and its molecular weight, it was possible to calculate the molar fractions of all the species. The resulting experimental distribution of reaction products for all the formulations are listed in Table 1. These values are in very good agreement with those expected for an ideal reaction. The results are consistent with FTIR measurements and confirm that no secondary reactions take place during reaction. Thus, the ring opening of the epoxy group with a carboxyl group is the main and only reaction.

Figure 5 shows X-ray diffraction experiments carried out for pure PA and PA-based precursors as prepared, i.e. after being cooled to room temperature. As prepared, PA1 crystallizes instantaneously while the crystallization of PA2 and PA4 needs time. Only the main lines diffracted with the corresponding intensity for pure PA are shown, in order to avoid crowding. PA1 and PA2 showed the same pattern, exhibiting two X-ray reflections at 7.17 and 21.45 2θ with corresponding d spacings of 12.35 and 4.22 Å, respectively. PA4 did not show any pattern as its crystallization rate is low. The weak signals for PA2 can be seen in the insets of Fig. 5. These results suggest the same ordering of the acyl chains for all the precursors. The diffraction peak located in the short spacing region match closely the one found for pure PA (4.19 Å), while the long d-spacing diffraction peak did not match the fatty acid pattern. This result is not surprising as it is well known that the long d spacing varies with the length of the chain from one member to the next by some increment which depends on the particular series.[19] The broad peak around 18 2θ is a clear sign of amorphous material. The amorphous behaviour is clearer for samples with less order due to mixing of compounds (PA4 > PA2 > PA1). Thus, PA4 is almost an amorphous material, while PA1 has some crystalline domains.

At the reaction temperature, the initial blends as well as the reaction products were homogeneous. After cooling to room tem-

Table 2. Thermal properties of polymer networks containing various contents of PA-based precursors

System	PA content (wt%)	Crystallinity (°C)	ΔH_c (J g^{-1})	Melting (°C)	ΔH_f (J g^{-1})	T_g (°C)
PA-based precursors						
PA1	59.5	22/30	68	33/50	72	–
PA2	42.2	16	48	25	50	–
PA4	26.7	13	37	18	36	–
Polymer networks						
TAZ-DGEBA-MXDA	–	–		–		106
PA1-TAZ-DGEBA-MXDA	10	7		34		104
PA1-TAZ-DGEBA-MXDA	20	11/23		33/47		94.5
PA2-TAZ-DGEBA-MXDA	10	10		33		82
PA2-TAZ-DGEBA-MXDA	20	13		32		73
PA4-TAZ-DGEBA-MXDA	10	–		–		64.5
PA4-TAZ-DGEBA-MXDA	20	–		–		36

perature, all formulations showed the presence of a crystalline phase. Table 2 shows crystallization and melting temperatures of the PA-based precursors obtained by DSC. The melting temperature of the ordered phase formed in PA-based precursors depends on the chain length of the components. Double endothermic peaks are only observed for PA1, as shown by the DSC traces in the upper right-hand corner in Fig. 6. This result could be related to the coexistence of two different crystal sizes in the solid state. These endothermic peaks change in sharpness and heat evolution with annealing at a temperature slightly below the second peak for about 30 min or at −20 °C for several days. Samples subjected to either of the thermal treatments show a very small peak at 33 °C and a sharp peak appearing at 50 °C. These observations suggest that the solid phase that melts at lower temperature is not stable and evolves to form part of the second population of crystals (T_m = 50 °C). The peak temperature of the transition for the monosubstituted component, PA4, is 18 °C. The corresponding thermogram for PA2 presents only one endothermic peak appearing at 25 °C. This behaviour suggests that the two components present in PA2 are mutually miscible in the solid phase. Probably, this mixing behaviour could be related to identical intermolecular interaction energies for mixed-pair (monosubstituted/disubstituted) and like-pair (monosubstituted/monosubstituted and disubstituted/disubstituted). The interaction between neighbouring molecules is mostly through van der Waals forces. As a result of participation of a number of individual atoms (forming the long chain of the molecule), the resultant van der Waals force acting between two adjacent molecules, mixed- or like-pair, should be similar. The reasons are that both molecules have the same acyl chain length and the connector in the disubstituted component is quite long. The cooling scans show only one sharp transition for PA2 and PA4. As expected, two crystallization peaks were observed for PA1 corresponding to the two crystal populations.

The heat of fusion expressed per unit mass of CH_2 groups supplied by PA may be compared with the value reported for the heat of fusion of polyethylene crystal, equal to 289 J g^{-1}.[20] Fig. 7 shows the percentage of CH_2 groups of fatty ester chains that could be crystallized for the different PA-based precursors (black symbols). The fraction of CH_2 groups that could be crystallized decreases from 78% in pure PA to 22% and 11% for PA1 and PA4, respectively. The decrease in crystallinity is associated with the difficulty in aligning the fatty ester chains for substituted species. The melting temperature also decreases on increasing the DGEBA/PA ratio.

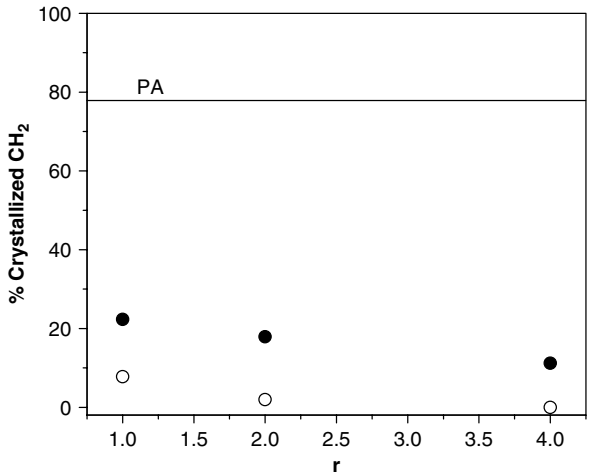

Figure 7. Percentage of CH_2 groups of the palmitic ester chain that could be crystallized in the reaction product as a function of the DGEBA/PA ratio for precursors (black symbols) and networks (white symbols). The corresponding value for pure PA is marked as a line.

Morphologies and thermal properties of polymer networks

Table 2 shows the thermal properties of all polymer networks. The thermal behaviour of the PA-TAZ-DGEBA-MXDA system revealed that the two crystal populations phase separate and crystallize during network formation when employing PA1 as modifier. Figure 6 shows the heating and cooling experiences of the PA1-based network with different thermal histories. The melting temperatures observed coincide with those determined for pure PA1. When using PA2 and PA4 as modifiers, the only component that crystallizes is the disubstituted one. One crystal population was observed that melts near 33 °C. The monosubstituted component which has epoxy groups capable of reacting with network precursors cannot crystallize. In the light of the experimental evidence, the PA tail connected to the gel by one reacted epoxy functionality has not enough mobility to be a part of the crystalline structure. As expected, the decrease in crystallinity is more pronounced comparing PA-modified networks

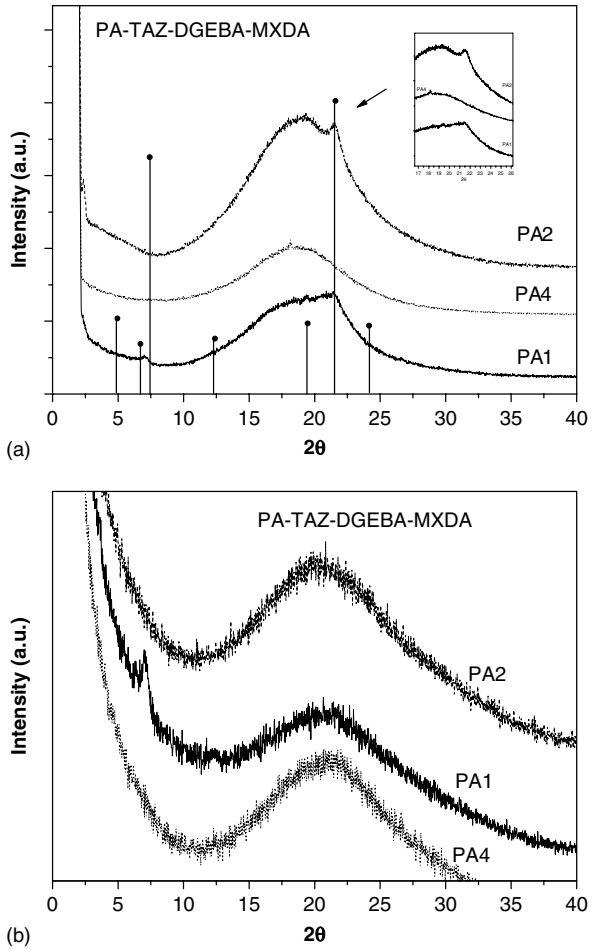

Figure 8. X-ray diffractograms for PA-TAZ-DGEBA-MXDA polymer networks containing 20 wt% PA based-precursors prepared (a) in bulk and (b) as thin films.

(white symbols, Fig. 7) with PA-based precursors (black symbols, Fig. 7).

The T_g dependence of the PA-TAZ-DGEBA-MXDA system on PA-based precursor stoichiometry exhibits a constant decrease as long as r increases. The reaction of the monosubstituted species present in PA-based precursors with amine groups during network formation reduces the crosslink density, and consequently it is expected to cause a decrease in the glass transition temperature. This means that the decrease in T_g generated by the modification of the network topology by reacting DGEBA with PA prevailed over the increase in T_g caused by the restriction of polymer chain motion produced by alkyl chain crystallization.

Figure 8 shows the X-ray diffractograms for the PA-TAZ-DGEBA-MXDA system. The figure also allows a comparison of the crystalline structure in the bulk and in thin films. Polymer networks containing PA1 and PA2 prepared in bulk showed the same pattern as the corresponding precursors, exhibiting two relevant X-ray reflections at 7.17 and 21.45 2θ with corresponding d spacings of 12.35 and 4.22 Å, respectively. The thermoset synthesized with PA4 in bulk did not show any diffraction peak, in good agreement with the DSC results. It can be seen that the crystalline structure in the long spacing region in thin films is maintained only for the PA1-modified polymer network.

The presence of a PA-based precursor modifies the phase behaviour of the system. In previous work, Fernández *et al.*[11] demonstrated that for the TAZ-DGEBA-MXDA system no phase separation occurred for several TAZ contents (up to 50 wt% TAZ). Morphologies generated in films synthesized using PA-based precursors are shown in Fig. 9. As the performance of the final material depends on the morphologies generated and their relationships with the required properties, it is important to analyse the factors involved in the phase separation process. The evolution of morphologies in the course of polymerization was followed by TOM. Phase separation was only observed for formulations containing PA1 and PA2. During curing of the PA-TAZ-DGEBA-MXDA system, the initially dissolved PA-based precursor and TAZ in the monomers phase separate due to an increase in the molecular weight of the thermosetting resin. These systems represent typical examples of a reaction-induced phase separation during step polymerization.[21] As result, co-continuous structures were generated over which surface crystal formation is observed (Figs 9(a) and 9(b)). The dark region is ascribed to the TAZ-rich phase, while the bright region corresponds to the epoxy-rich phase. Both phases remained stable, exhibiting a relatively uniform characteristic size. The observed morphologies did not change after prolonged periods of storage (several weeks), at $-20\,^{\circ}C$ or at room temperature, but crystals were observed to migrate to the surface. For the PA1-TAZ-DGEBA-MXDA system, the same formulation was cured inside two glass plates to avoid crystal migration towards the surface. It was found that crystals are located in the epoxy-rich phase. The PA1 dissolved in the epoxy-rich phase after the first phase separation process suffers an additional phase separation during the cooling stage.

For the PA4-TAZ-DGEBA-MXDA system (Fig. 9(c)), no phase separation was observed. When cooling these solutions the system evolved from a rubbery to a glassy homogeneous gel. An inspection of the micrograph after 2 weeks of storage at room temperature highlights surface crystal formation. A possible explanation is the presence of crystals of the disubstituted product PA-DGEBA-PA, as the experimental proportion of this component was 0.04 (Table 1).

Photoinduced birefringence in polymer networks

Measurement of photoinduced birefringence offers a bulk probe for various motions occurring in the sample. To understand the mobility of the azo chromophore in the polymer network and clarify the effect of organic crystals on the orientation behaviour, *in situ* birefringence measurements were performed during writing cycles (linearly polarized pump on), relaxation cycles (pump off) and photoinduced erasing processes (circularly polarized pump on). Optical characteristics for all network series are listed in Table 3.

The level of maximum birefringence that can be achieved was about 0.0100 for the reference polymer TAZ-DGEBA-MXDA, which is the expected value according to the low chromophore concentration (5 wt% DO3).[7] The value of the induced anisotropy for PA1-modified networks is comparable with the reference polymer and slightly higher than those obtained for networks synthesized with PA2 and PA4. This is an indication that, for the networks analysed here, the maximum induced birefringence is only a function of the overall chromophore concentration. These experimental results are consistent with those reported by Takase *et al.*[22] comparing the maximum birefringence of azo-containing polymethacrylate copolymers before and after crosslinking. They found that the maximum value achieved during the linearly polarized laser irradiation is only a function of the azo content.

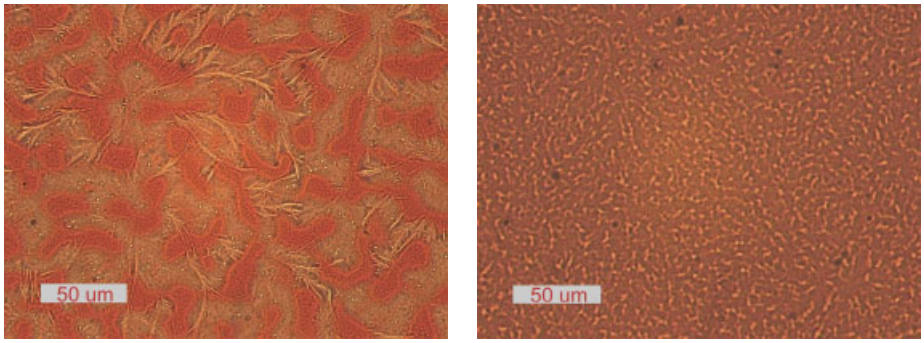

(a) (b)

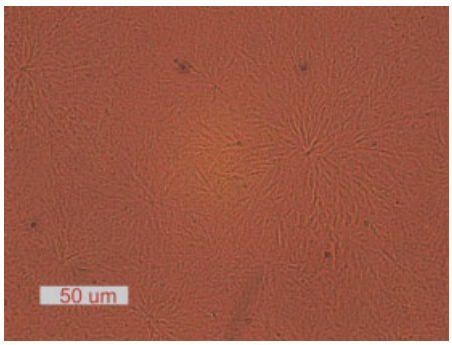

(c)

Figure 9. TOM micrographs of polymer networks containing 20 wt% PA-based precursors after complete reaction: (a) PA1-TAZ-DGEBA-MXDA after cooling from 100 °C; (b) PA2-TAZ-DGEBA-MXDA after cooling from 100 °C; (c) PA4-TAZ-DGEBA-MXDA obtained after 2 weeks of storage at room temperature.

Table 3. Optical characteristics of polymer networks modified with PA-based precursors

System	PA content (wt%)	Δn	Remnant birefringence (%)
TAZ-DGEBA-MXDA	0	0.0097	50
PA1-TAZ-DGEBA-MXDA	10	0.0100	50
PA1-TAZ-DGEBA-MXDA, annealed[a]	10	0.0097	54
PA1-TAZ-DGEBA-MXDA	20	0.0096	56
PA1-TAZ-DGEBA-MXDA, annealed[a]	20	0.0096	60
PA2-TAZ-DGEBA-MXDA	10	0.0085	23
PA2-TAZ-DGEBA-MXDA, annealed[a]	10	0.0077	44
PA2-TAZ-DGEBA-MXDA	20	0.0082	17
PA2-TAZ-DGEBA-MXDA, annealed[a]	20	0.0074	31
PA4-TAZ-DGEBA-MXDA	10	0.0081	17
PA4-TAZ-DGEBA-MXDA, annealed[a]	10	0.0078	20
PA4-TAZ-DGEBA-MXDA	20	0.0076	14
PA4-TAZ-DGEBA-MXDA, annealed[a]	20	0.0074	22

[a] Samples annealed at −20 °C for 14 days.

Figure 10 shows the time evolution of the photoinduced birefringence for PA-modified networks. In order to examine the annealing effect on their optical behaviour, the figure also shows the optical response for samples with different thermal histories. No transmission of the probe beam, which passed through two crossed polarizers placed before and after the film, was observed, indicating the random orientation of the chromophores. However, when the writing beam was turned on at point A, the transmission increased because of the induced birefringence in the film. When the writing beam was turned off at point B, birefringence levels fell off from the saturation level to a relaxed level (point C). The induced birefringence could be optically erased by overwriting the test spot with circularly polarized laser light that randomized the chromophores' orientation, thereby eliminating the macroscopic dipole orientation. This writing–erasing cycle can be repeated many times on the same spot on the polymer film, achieving the same level of birefringence at the same rate.

The results depicted in Fig. 10 and Table 3 demonstrate that the optical response, more specifically the remnant anisotropy, is a direct consequence of the morphologies generated and that crystallization can take place. When the PA-based precursor is not

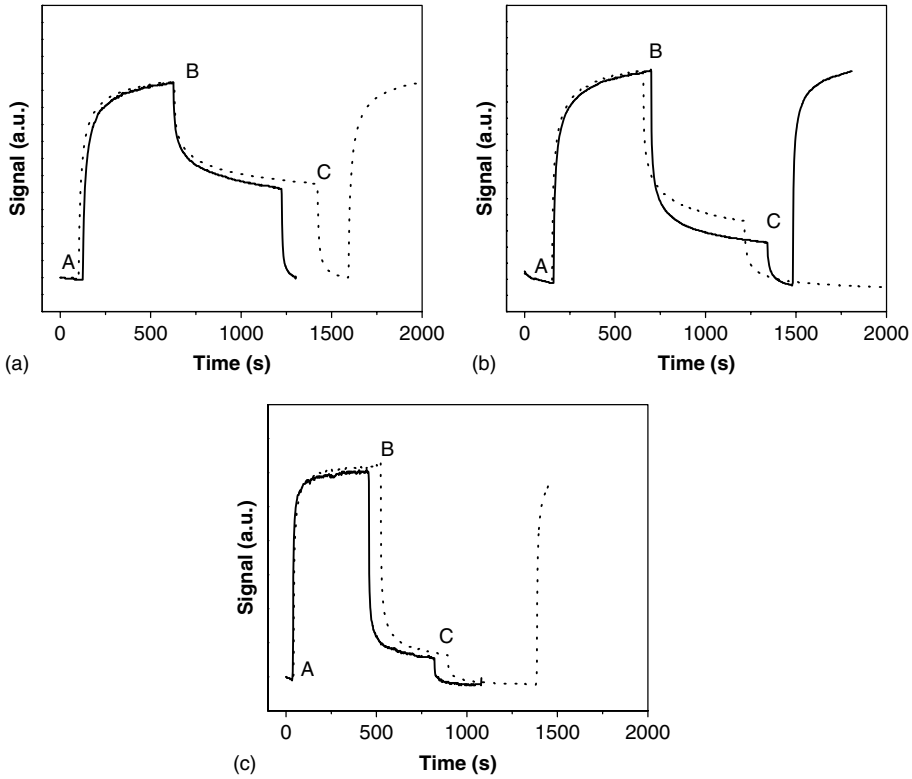

Figure 10. Writing, relaxing and erasing sequences in the PA-TAZ-DGEBA-MXDA system with (a) PA1, (b) PA2 and (c) PA4. The figure shows the optical response for samples with different thermal histories: annealed at −20 °C for 14 days (dotted lines) and after being cooled from 100 °C (solid lines).

covalently bonded to the matrix, e.g. PA1 that contains 87% of the disubstituted product, it can crystallize easily. Samples with different thermal histories show similar behaviour as shown in Fig. 10(a). This means that the migrated crystals over the surface do not take part in the photoresponse. This system also shows an optical response similar to the reference network, TAZ-DGEBA-MXDA (see Table 3). This behaviour is consistent with the fact that PA1 and TAZ are located in different phases.

As shown in Fig. 10(c), PA4-modified materials present a completely different response. The signal decays almost completely at point B, showing a behaviour that could be of great importance in the development of optical switches. In this case, the dissolved organic tails in the matrix are unable to crystallize. The observed behaviour is probably related to an important decrease in the glass transition temperature caused by crosslink density reduction during curing (Table 2). The lower the T_g value, the higher the molecular mobility is and the lower the remnant birefringence. In addition, it is interesting to note that the curves obtained for the samples subjected to either of the thermal treatments are very similar. These results are as expected, taking into account that the proportion of disubstituted product in PA4 is negligible.

PA2-modified materials show an intermediate behaviour compared with PA1- and PA4-based epoxy networks (Fig. 10(b) and Table 3). With increasing PA2 concentration from 10 to 20 wt%, a decrease in the remaining birefringence is observed (from 23% to 17%) and a consequent decrease in T_g value (from 82 to 73 °C). Formulations containing a constant PA2 concentration but different thermal history exhibit variable remnant birefringence. The remaining birefringence is approximately double after annealing. This tendency is probably related to the presence of dispersed crystal domains, which act as anchoring points reducing the mobility of azobenzene chains in the matrix. Higher crystal domains restrain the mobility of oriented azo groups for randomization.

So, we have to conclude that the photo-orientation of the azo chromophores is influenced by (a) the morphology of the system and (b) the crystalline arrangement of the molecules and thus the aggregation and local free volume distribution around the chromophores. As we have previously mentioned, the level of maximum birefringence that can be achieved for all the systems analysed was as expected, according to the chromophore concentration. This means that the reorientation of the whole of the semicrystalline domains located on the surface to a direction perpendicular to the light polarization did not happen. Probably, cooperative motion is driven by the polar interaction between azo and non-azo semicrystalline domains. Natansohn *et al*.[23] reported a systematic study of the cooperative motion in the amorphous phase by investigating two copolymer pairs. By changing the polarity of the azo and non-azo structural unit they demonstrated that cooperative motion was only observed for polar–polar pairs.

CONCLUSION

In this study we discuss the synthesis and possible applications of new optically active polymeric networks containing azobenzene moieties and different alkyl compounds. Several crosslinked epoxy-based azopolymers containing various PA-based precursor contents and constant chromophore concentration equal to 5 wt% DO3 were synthesized. It was possible to develop materials with a variable optical response.

Different morphologies could be obtained in epoxies modified simultaneously with TAZ and PA-based precursors. The lack of compatibility induces phase separation of TAZ-rich and

epoxy/amine-rich phases. Phase separation was only observed for formulations containing PA1 and PA2. During curing, the initially dissolved PA-based precursor and TAZ in the monomers phase separate due to an increase in the molecular weight of the thermosetting resin. These systems represent typical examples of a reaction-induced phase separation during step polymerization.

Measurements of the birefringence (Δn) induced with linearly polarized 488 nm light show that networks with the same chromophore concentration but modified with various PA-based precursor concentrations exhibit similar levels of induced anisotropy under the same irradiation conditions. Their reversible optical storage properties were studied and compared. It was found that the remnant anisotropy is a direct consequence of the morphologies generated and the crosslinking density of the networks, and that crystallization of PA-based precursor can take place. When the PA-based precursor is not covalently bonded to the matrix, e.g. PA1, the high remaining birefringence fraction makes these materials promising for optical storage applications, waveguides and second harmonic generation.

PA4-modified materials present a completely different response, showing a behaviour that could be of great importance in the development of optical switches. In this case, the dissolved organic tails in the matrix are unable to crystallize, giving a typical 'on–off' response. PA2-modified materials show an intermediate behaviour compared with PA1- and PA4-based epoxy networks. Formulations containing a constant PA2 concentration but different thermal histories exhibit variable remnant birefringence.

ACKNOWLEDGEMENTS

The authors are grateful for the financial support of the University of Mar del Plata, CONICET and ANPCyT (Argentina). We acknowledge the excellent comments and suggestions received from the two reviewers that significantly improved the manuscript.

REFERENCES

1 Ho CH, Yang KN and Lee SN, *J Polym Sci Polym Chem* **39**:2296 (2001).
2 Cui L, Tong X, Yan X, Liu G and Zhao Y, *Macromolecules* **37**:7097 (2004).
3 Kim TD, Lee KS, Lee GU and Kim OK, *Polymer* **41**:5237 (2000).
4 Xinlin T, Zhen C, Lifeng W, Xiaogong W and Deshan L, *Polym Prepr* **41**:1405 (2000).
5 Meng X, Natansohn A, Barrett C and Rochon P, *Macromolecules* **29**:946 (1996).
6 He Y, Wang H, Tuo X, Deng W and Wang X, *Opt Mater* **26**:89 (2004).
7 Eich M, Wendorff J, Reck B and Ringadorf H, *Makromol Chem Rapid Commun* **8**:59 (1987).
8 Tredgold R, Allen R, Hodge P and Khoebdel E, *J Phys Appl Phys* **20**:1385 (1987).
9 Natansohn A and Rochon P, *Chem Rev* **102**:4139 (2002).
10 Fernández R, Mondragón I, Galante MJ and Oyanguren PA, *J Polym Sci Polym Phys* **47**:1004 (2009).
11 Fernández R, Mondragon I, Oyanguren PA and Galante MJ, *React Funct Polym* **68**:70 (2008).
12 Fernández R, Mondragon I, Galante MJ and Oyanguren PA, *Eur Polym J* **45**:788 (2009).
13 Fernández R, Blanco M, Galante MJ, Oyanguren PA and Mondragon I, *J App Polym Sci* **112**:2999 (2009).
14 Kern W, *Semicond Int* **7**:94 (1984).
15 Sáiz LM, Orofino AB, Ruzzo MM, Arenas GF, Oyanguren PA and Galante MJ, *Polym Int* **60**:1053 (2011).
16 Tess RW, in Epoxy Resin Coatings *Epoxy Resins Chemistry and Technology*, ed. by May CD. Marcel Dekker, New York, pp. 719–782 (1988).
17 Schechter L and Wynstra J, *Ind Eng Chem* **48**:86 (1956).
18 Socrates G, in *Infrared Characteristic Group Frequencies*. John Wiley, Chichester, The carbonyl group (1994).
19 Abes M and Narine SS, *Chem Phys Lipids* **149**:14 (2007).
20 Quinn FA Jr and Mandelkern L, *JACS* **80**:3178 (1958).
21 Williams RJJ, Rozenberg BA and Pascault JP, *Adv Polym Sci* **128**:95 (1997).
22 Takase H, Natansohn A and Rochon PJ, *J Polym Sci Polym Phys* **39**:1686 (2001).
23 Natansohn A, Rochon P, Meng X, Barrett C, Buffeteau T, Bonenfant S, *et al*, *Macromolecules* **31**:1155 (1998).

